Int. J. Heat Mass Transfer. Vol. 36, No. 17, pp. 4133–4139, 1993
Printed in Great Britain

0017-9310/93 $6.00+0.00
Pergamon Press Ltd

Evaporative cooling due to a gently deposited droplet

M. DI MARZO, P. TARTARINI and Y. LIAO
Mechanical Engineering Department, University of Maryland, College Park, Maryland 20742, U.S.A.

and

D. EVANS and H. BAUM
Building and Fire Research Laboratory, National Institute of Standards and Technology, Gaithersburg, Maryland 20899, U.S.A.

(*Received* 9 *March* 1993 *and in final form* 21 *May* 1993)

Abstract—The transient thermal behavior of a single water droplet gently deposited on the surface of a semi-infinite solid is investigated. A coupled model that solves simultaneously the transient conduction equation for the solid and the liquid to yield the surface temperature and heat flux distributions as well as the description of the droplet evaporation transient is proposed. The predictions of the evaporation time are compared with experimental data. An additional model is presented which assumes constant heat flux at the liquid–solid interface. This model provides a closed form solution for the solid surface transient temperature distribution.

INTRODUCTION

THE COOLING of hot solid surfaces by droplet evaporation has been studied extensively. Multi-droplet systems were investigated both theoretically and experimentally over several years; see for example the work of Toda [1], Bonacina *et al.* [2] and Tio and Sadhal [3]. Single droplet systems were described by Inada *et al.* [4], Makino and Michiyoshi [5, 6] and Takano and Kobayashi [7] among others.

The droplet configuration upon impacting a solid surface has been discussed in great detail by Chandra and Avedisian [8] while the droplet shape during the last stages of evaporation was examined by Zhang and Yang [9].

In this paper general models are derived for the case of a water droplet gently deposited over the surface of a semi-infinite solid. A typical photographic description of the evaporative transient, which is consistent with a similar record provided by Xiong and Yuen [10], is shown in Fig. 1. The initial solid surface temperature is below the limit at which onset of nucleate boiling is observed. The formulation of a model to predict both the evaporation time and the transient thermal behavior of the solid surface is the first step in formulating more comprehensive predictive tools for multi-droplet evaporative cooling.

The transient thermal behavior of a high conductivity semi-infinite solid has been modeled by imposing a constant uniform temperature at the solid–liquid interface [11, 12]. The models based on this assumption yield good predictions for cases where the surface temperature is not experiencing major changes during the process which is most common for high thermal conductivity solids. However, these models are unable to predict the solid thermal behavior for low thermal conductivity materials which exhibit large temperature variations during the drop evaporating process. De-coupling the liquid from the solid (by imposing that artificial boundary condition at the solid–liquid interface) means that the liquid droplet is assumed to behave independently of the substrate (i.e. the solid). The interfacial temperature at the initial liquid–solid contact is approximated by the exact solution available for the contact temperature of two semi-infinite solids. Seki *et al.* [11] based their analysis on this consideration and suggested that the interfacial temperature can be obtained as:

$$T_c = \frac{T_l\sqrt{(\rho_l c_l k_l)} + T_s\sqrt{(\rho_s c_s k_s)}}{\sqrt{(\rho_l c_l k_l)} + \sqrt{(\rho_s c_s k_s)}}. \quad (1)$$

The constant temperature model does not conserve energy at the liquid–solid interface since there is no energy conservation constraint. This constitutes a major barrier to the extension of these results to the multi-droplet formulation because the overall heat balance for multiple droplet solid cooling cumulates the single droplet inaccuracies.

THEORETICAL MODELS

Coupled model description

Inspection of Fig. 1 reveals that the liquid–solid receding angle (which has been found to be 7° for aluminum and water) is reached when a small fraction of the original water in the droplet is left [13]. Therefore, it is reasonable to assume that the surface of the wetted area is constant throughout the evaporative process as can be deduced from the figure.

Visual inspection of a tracer and the measurements reported by Ostrach and Pradhan [14] indicate that

NOMENCLATURE

c	specific heat
d	diameter of the wetted region
D	air-steam mass diffusivity
erf	error function
G	Green's function; see equation (12)
h	overall heat transfer coefficient
h_{conv}	convective heat transfer coefficient
J_0, J_1, I_0	Bessel's functions
JA	Jakob number; see equation (20)
k	thermal conductivity
L_0	modified Bessel's function, $e^{-\zeta}I_0(\zeta)$
q	heat flux
q_τ	reference heat flux, $\Lambda\rho_l V_l'/(\pi R^2\tau)$
r	radial coordinate
R	radius of the wetted area; see Fig. 2
S	surface; see equation (15)
t	time
T	temperature
T_c	contact temperature; see equation (1)
u	transformed temperature; see equation (13)
V	droplet volume or volume; see equation (15)
x	molar fraction of steam in air
z	axial coordinate.

Greek symbols

α	thermal diffusivity
β	shape parameter; see equation (19)
δ	normalized time, $(\alpha_s t)^{1/2}/R$
δ_τ	normalized evaporation time, $(\alpha_s\tau)^{1/2}/R$
ζ, λ	dummy variables
η	normalized radius, r/R
η_ϕ	radius of influence associated with the constant ϕ
θ	normalized temperature; see equation (17)
Λ	liquid latent heat of vaporization
ρ	density
τ	total evaporation time
ϕ	arbitrary constant.

Subscripts

a	far-field air property
i	liquid–vapor interfacial property
l	liquid property at the liquid–solid interface
o	solid initial property
s	solid surface property
*	Green's function argument; equations (12) and (14).

little convective motion is present in the water droplet. Therefore, one can assume that the dominant mechanism of heat transfer in the water droplet is conduction. This assumption is common to most previous models [1, 11, 12, 15]. The shape of the water droplet in Fig. 1 can be described with good approximation as a segment of a sphere of fixed base and decreasing apex [12]. This geometrical representation of the deposited droplet is accurate while the liquid–solid contact angles exceeds the receding angle [13] as previously discussed. The modeling of the coupled solid and liquid thermal behavior is described by the transient conduction equation for both domains with the appropriate boundary conditions.

The governing equations, with respect to the coordinate system depicted in Fig. 2, are:

$$\frac{\partial T}{\partial t} = \alpha_s\nabla^2 T, \quad \frac{\partial T}{\partial t} = \alpha_l\nabla^2 T. \qquad (2, 3)$$

The initial and boundary conditions are as follows:

$$\text{at } t = 0, \quad \text{for the solid}: \quad T = T_0 - \frac{q_o z}{k_s}$$

$$\text{and for the liquid}: \quad T = T_a \qquad (4, 5)$$

at $0 \leqslant r \leqslant R$, $z = 0$:

$$T_s = T_l, \quad k_s\left(\frac{\partial T}{\partial z}\right)_s = k_l\left(\frac{\partial T}{\partial z}\right)_l$$

at $r > R$, $z = 0$:

$$k_s\left(\frac{\partial T}{\partial z}\right)_s = h(T_s - T_a) \qquad (6, 7, 8)$$

at $z \to -\infty$ for all r's

$$-k_s\left(\frac{\partial T}{\partial z}\right)_s = q_o$$

at $r \to \infty$, $z \leqslant 0$:

$$\left(\frac{\partial T}{\partial r}\right)_s = 0. \qquad (9, 10)$$

At the liquid–vapor interface, a small portion of the heat conducted from below through the liquid is transferred to the ambient by convection and by radiation. Most of the heat evaporates the liquid.

The conservation of energy at the liquid–vapor interface provides the remaining boundary condition needed for equation (3). To account for the evaporation, the vapor diffusion in the air is considered. Details of the derivation of this liquid–vapor interfacial condition are given by di Marzo and Evans [12]. In the derivation the mass transfer coefficient is related to the convective heat transfer h_{conv} by the Chilton–Colburn analogy [16].

The final formulation of the boundary condition at the liquid–vapor interface can be written as:

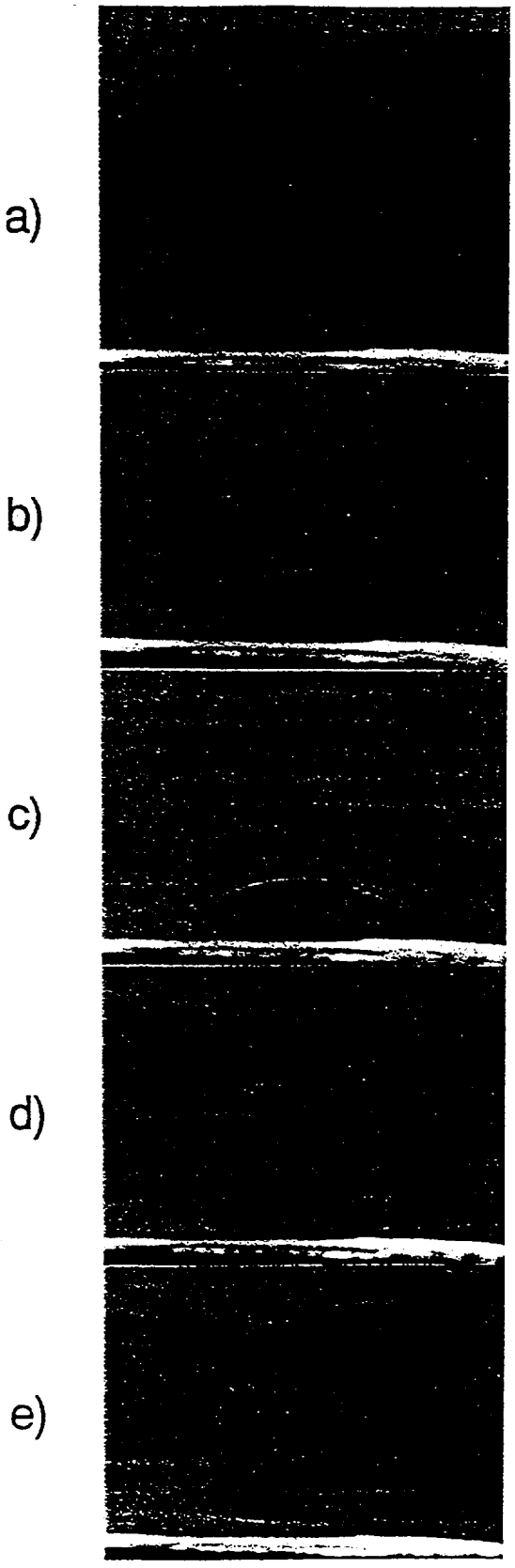

FIG. 1. Typical photographic record of a 30 μl droplet on aluminum ($T_s = 92$ C, $\tau = 86$ s) at (a) $t/\tau = 0$; (b) $t/\tau = 0.21$; (c) $t/\tau = 0.38$; (d) $t/\tau = 0.62$ and (e) $t/\tau = 0.85$.

$$-k_l \nabla T \cdot \hat{n} - h(T_i - T_a) = 0.624 h_{conv} \left(\frac{D}{\alpha_a}\right)^{2/3} \frac{\Lambda}{c_a} \frac{x_i - x_a}{1 - x_a} \quad (11)$$

where the temperature gradient is taken normal to the liquid vapor interface. The grid geometry shown in Fig. 2 is such that this gradient is normal to the upper boundary of the computational domain for the liquid region.

Extremely strong local thermal gradients at the droplet edge, during the initial transient, pose some difficulties to the solution of this problem with conventional finite difference schemes. In the present study, the solution of the transient conduction equation in the solid is obtained by using a Boundary Element Method (BEM). This is combined with a finite volume treatment of the liquid droplet. The BEM is described in detail by Kavoosi *et al.* [17]. The adjoint equation to equations (2) is satisfied by the following Green's function [18]:

$$G(r, z, t; r^*, z^*, t^*) = (4\pi\alpha_s t^*)^{-3/2} \times \left\{e^{-[(r-r^*)^2+(z-z^*)^2]/(4\alpha_s t^*)} + e^{-[(r-r^*)^2+(z+z^*)^2]/(4\alpha_s t^*)}\right\}. \quad (12)$$

A linear combination of equation (2) and of its adjoint equation, is integrated over the solid and temporal domain. By applying the Gauss theorem on the volume integral, one obtains the following relationship between the solid temperature and its normal derivative at the solid surface:

$$u(r, t) = T - T_s - \frac{q_0 z}{k_s} = \int_0^t \int_0^\infty \nabla u(r^*, t^*) r^* t^{*-3/2} L_0\left(\frac{2rr^*}{4\alpha_s t^*}\right) \times e^{-(r-r^*)^2/(4\alpha_s t^*)} \, dr^* \, dt^*. \quad (13, 14)$$

The governing equation for the liquid is cast in the following form:

$$\int_v \frac{\partial T}{\partial t} \, dv = \alpha_l \int_S \nabla T \cdot \hat{n} \, ds \quad (15)$$

which is integrated for each elementary volume of the discretized liquid domain. The volume elements are defined in terms of the coordinates shown in Fig. 2. Details on the treatment of the liquid domain are given by Liao [19]. These two equations, equations (14) and (15), represent the energy conservation in the solid and liquid respectively. In their discretized form they become matrix equations for the transient temperature and heat flux distribution in the liquid and over the solid surface.

A computer code has been developed to solve these equations [19]. The input to the code must prescribe: (a) the droplet initial volume; (b) the droplet shape parameter β as defined by Bonacina *et al.* [2]; (c) the initial surface temperature; (d) the overall heat transfer coefficient and (e) the convective heat transfer

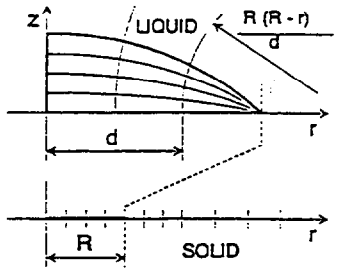

FIG. 2. Coordinate system and nodalization.

coefficient. The shape parameter and the two heat transfer coefficients are provided by correlations based on experimental data. The code predicts: (a) the transient temperature profiles on the solid surface and throughout the liquid; (b) the heat fluxes at all points of the liquid domain and on the solid surface; (c) the total evaporation time and (d) the transient liquid inventory.

The shape parameter is reported for various solid materials and evaporating fluids by several investigators [2, 8, 12, 20]. The overall heat transfer coefficient has been measured by Klassen and di Marzo [21] and correlations are available in the literature to estimate the convective heat transfer coefficient.

Constant flux model

This model is of interest because its relative simplicity makes it a candidate for use in multi-droplet evaporative cooling studies. Carslaw and Jaeger [22] show that, for a semi-infinite solid with a surface heat flux constant and uniform applied over a disk of radius R and no heat transfer on the remainder of the surface, the transient temperature profile on the solid surface is given by

$$T_o - T_s = \frac{q_r R}{k_s} \int_0^\infty J_0(\lambda r) J_1(\lambda R) \operatorname{erf}\left(\lambda \sqrt{(\alpha_s \tau)}\right) \frac{d\lambda}{\lambda}. \tag{16}$$

By introducing the normalized radius $\eta = r/R$ and the normalized evaporation time $\delta_r = (\alpha_s \tau)^{1/2}/R$ and by setting q_r equal to the spatial and temporal averaged heat flux due to droplet evaporation, one obtains:

$$0 = JA \left(\frac{\rho_s}{\rho_l}\right) \delta_r^2 \beta^3$$

$$= \frac{4}{3} \int_0^\infty J_0(\zeta\eta) J_1(\zeta) \operatorname{erf}(\zeta\delta) \frac{d\zeta}{\zeta} \tag{17, 18}$$

where β is the shape parameter defined by Bonacina *et al.* [2] and JA is the Jakob number. These two parameters can be expressed as follows:

$$\beta = R\left(\frac{4\pi}{3V_l}\right)^{1/3}, \quad JA = \frac{c_s(T_0 - T_s)}{\Lambda}. \tag{19, 20}$$

In order to quantify the extent of the solid surface region affected by the droplet cooling, a significant parameter is the radial heat flux at the surface at any given location. The presence of the droplet is felt when this radial heat flux is greater than a fraction of the reference value identified as the spatial and temporal averaged heat flux, that is:

$$k_s \frac{\partial T_s}{\partial r} \geqslant \phi \frac{\Lambda \rho_l V}{\pi R^2 \tau}. \tag{21}$$

By using equations (18) and (19), this condition, in terms of normalized quantities, becomes:

$$-\frac{\partial \theta}{\partial \eta} \geqslant \frac{4}{3}\phi$$

$$\int_0^\infty J_1(\zeta\eta) J_1(\zeta) \operatorname{erf}(\zeta\delta)\, d\zeta \geqslant \phi \tag{22, 23}$$

where ϕ is an arbitrary constant. Equation (23) can be used to define the radius of influence η_ϕ $(= r_\phi/R)$ as the minimum value of η that satisfies the inequality. The radius of influence can be defined for $\phi = 0.1$ which relates the radial heat flux to 10% of the spatial and temporal averaged heat flux (see equation (21)). With this definition one implies that a radial heat flux of less than 10% of the reference heat flux is considered small. At such distance from the droplet and beyond, the evaporative cooling effect is considered equally small. Note that the definition of the radius of influence is based on the arbitrary constant ϕ. Therefore, it can be used only on a comparative basis.

MODELS VALIDATION

Coupled model

A comparison of the coupled model with the experimental data is obtained by looking at the evaporation times for aluminum [12] and for macor [20]. Figure 3 shows the calculated and measured evaporation time for both materials for various initial solid surface temperatures and droplet sizes. The agreement is

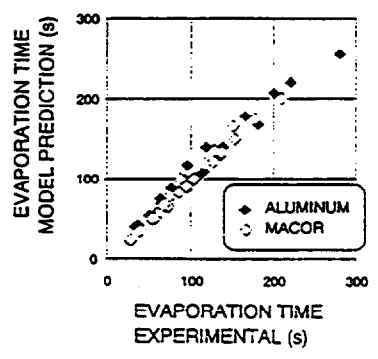

FIG. 3. Model validation: total evaporation time for droplets with $V = 10, 30, 50\ \mu l$ on aluminum with $T_s = 75$–102 C and on macor with $T_s = 101 \div 208$ C (data for aluminum from ref. [12], data for macor from ref. [20]).

remarkable in light of the fact that the experimental data are repeatable within 10% of the indicated value.

The cooling effect, due to the droplet, is strongly dependent on the properties of the solid. Figure 4 illustrates this point by comparing the temperature distributions for a 30 μl droplet which evaporates in 95 s on aluminum and macor. To achieve the same time averaged heat flux, the initial surface temperatures are obviously different: for aluminum $T_s = 91°C$ and for macor $T_s = 119°C$. The curves shown in the figure are at 29 and 86 s after deposition. Note the minimal temperature excursion for aluminum and the rather deep temperature drop for macor. Further, the cooling effect is felt over a large portion of the aluminum surface (more than nine droplet radii) while the effect is rather contained on the macor surface (about three droplet radii) albeit much more intense. The other aspect, that emerges from the analysis of the code computation, is the unidimensionality of the heat transfer in the liquid region. The radial heat flux, at various locations and at various stages of the evaporative process, amounts to less than 5% of the total heat flux in most cases. Only for a few locations at the droplet edge, for low thermal conductivity materials, toward the end of the process, does its contribution exceed 10% of the total heat flux. This observation allows the simplifications of the model for the liquid layer, which will be particularly important in future studies of multi-droplet heat transfer.

The measured transient temperature distribution over the solid surface is illustrated in Fig. 5. These data are obtained via infrared thermography of the surface by Klassen *et al.* [20]. The temperature profiles shown in the figure are over a line (on the solid surface) passing through the center of the wetted region. The readings over the surface covered by the liquid

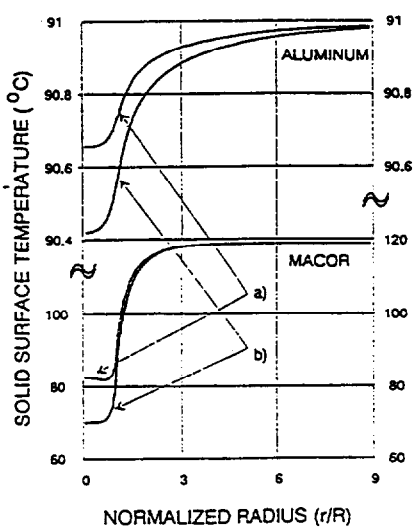

FIG. 4. Typical solid surface temperature profiles for a water droplet ($V = 30$ μl, $\tau = 95$ s) deposited on aluminum ($T_s = 91$ C) and macor ($T_s = 119$ C) for (a) $t/\tau = 0.3$ and (b) $t/\tau = 0.9$.

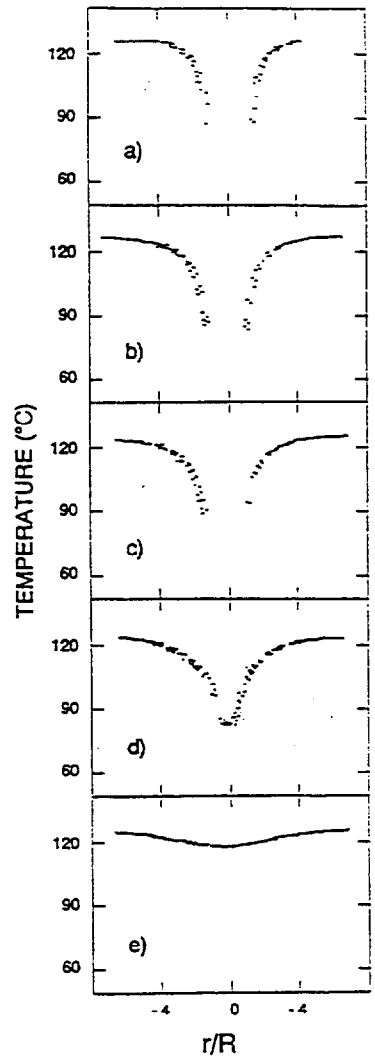

FIG. 5. Typical surface temperature distribution for a 30 μl droplet on macor (data from ref. [20] for $T_s = 124°C$ and $\tau = 100$ s) at (a) $t/\tau = 0.1$; (b) $t/\tau = 0.7$; (c) $t/\tau = 0.9$; (d) $t/\tau = 1.0$ and (e) $t/\tau = 1.1$.

(i.e. plots a, b, c for $r/R < 1$) cannot be related to a temperature scale due to the infrared radiation absorption of the water layer. Note that the last two plots (i.e. plots d, e) describe the surface temperature after the complete droplet vaporization.

Figure 6 compares the experimental data (shown as shaded regions) with the models previously described. Case (a) shows the results of the coupled model: case (b) illustrates the predictions of the constant flux model while case (c) is related to previous simplified models reported in the literature [11, 12].

The overall performance of the coupled model is quite reasonable. It slightly over-predicts the data while capturing well the temperature at the droplet edge ($r = R$). The radius of influence is under-estimated by this model. Both the droplet evaporation and the solid cooling are modeled and the simultaneous thermal transient description is obtained.

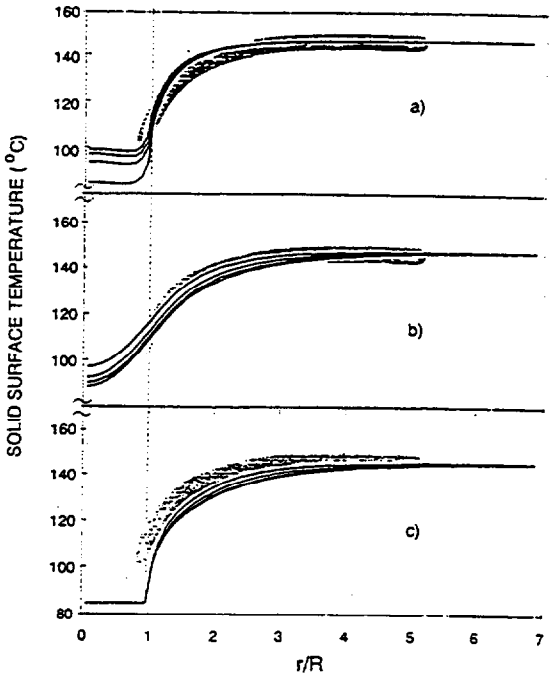

FIG. 6. Typical solid surface temperature profiles for droplets deposited on macor compared with data from ref. [21] with $0.3 \leqslant t/\tau \leqslant 0.9$ for (a) the coupled model; (b) the constant flux model and (c) the constant temperature model ($V = 30$ μl; $T_s = 145°C$; at $t/\tau = 0.3$; $t/\tau = 0.5$; $t/\tau = 0.7$ and $t/\tau = 0.9$).

Constant flux model

The constant flux model is able to predict the data well as shown in Fig. 6 (case b) where it slightly under-predicts the measured temperature profile while preserving the general trends. This closed-form solution over-estimates the droplet cooling effect.

Figure 7 shows the liquid–solid interfacial fluxes, calculated from the coupled model, for a typical case. It is important to note that the heat flux is not uniform nor constant during the evaporative process. The spatial distribution indicates that most of the evaporation takes place at the outer edge of the droplet. Therefore, it is not surprising that the constant heat flux model exhibits some discrepancies with the data for the temperature gradient at $r = R$ (or, in non-dimensional variables, for $\eta = 1$) as it can be seen in Fig. 6.

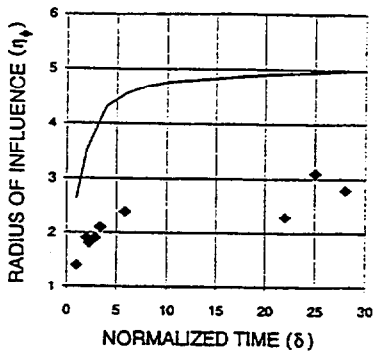

FIG. 8. Radius of influence vs normalized time with $\phi = 0.1$: —— constant flux model; ◆ coupled model.

The constant flux model provides a very good quantitative representation of the temperature profiles on the solid surface. However, it fails to capture the qualitative details of the transient behavior. Figure 5 shows that the measured temperature profile is almost constant throughout the process after a rapid initial transient. This behavior is well represented by the coupled model while the constant flux model exhibits an ever changing temperature profile as time progresses.

Concerning the cooling effect, the solution of equation (23), for $\phi = 0.1$, is shown in Fig. 8. The predictions of the coupled model, at selected values, are also shown in the figure for comparison. By inspecting Fig. 6, one can conclude that the actual radius of influence lies between the predictions of the coupled model and of the constant flux model. Note that the cylindrical coordinate system will favor the coupled model when the area of the surface influenced by the droplet is compared.

The fundamental difference between the coupled

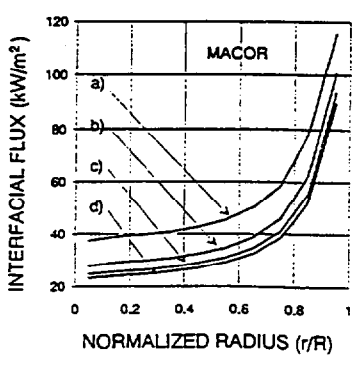

FIG. 7. Liquid–solid interfacial fluxes for water droplet with $V = 30$ μl on macor with $T_s = 145°C$ at (d) $t/\tau = 0.3$; (c) $t/\tau = 0.5$; (b) $t/\tau = 0.7$; (a) $t/\tau = 0.9$ and $\tau = 64$ s (coupled model computations).

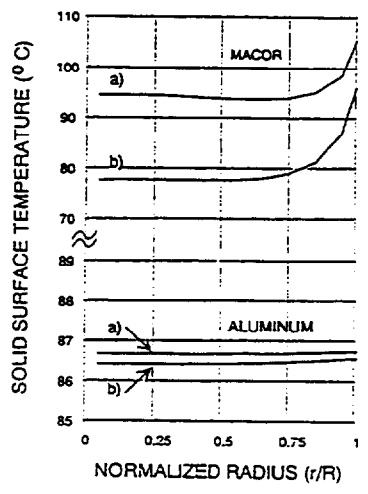

FIG. 9. Typical liquid–solid interfacial temperatures for macor and aluminum with $T_c = 82°C$ for water droplets with $V = 30$ μl at (a) $t/\tau = 0.3$ and (b) $t/\tau = 0.9$ (coupled model computations).

model and the constant flux model is in that *the coupled model provides a complete description of the phenomena while the constant flux model requires the droplet evaporation time (as an independent input) in order to estimate the spatial and temporal averaged heat flux* q_e.

Finally, the model based on the constant and uniform temperature at the solid–liquid interface underpredicts the surface temperature while over-predicting the surface cooling. Figure 9 illustrates the transient temperature distribution (obtained with the coupled model) at the liquid–solid interface for aluminum and macor when a 30 μl droplet is deposited on the solid with an initial solid surface temperature (T_s) which will yield a calculated contact temperature $T_c = 82°C$ from equation (1). As one can readily observe, this calculated contact temperature has no relation with the results shown in Fig. 9 since the solid–liquid interfacial temperature is changing with time as well as spatially.

CONCLUSIONS

This paper briefly reviews the formulation of two models for the prediction of the thermal behavior of the droplet–solid interaction during evaporative cooling. The coupled model, which solves simultaneously the liquid and the solid transient conduction equations, is validated over a wide range of parameters.

The constant flux model is also described. This model de-couples the liquid from the solid by introducing a simplified boundary condition at the liquid–solid interface (i.e. constant and uniform heat flux). A comprehensive discussion of the two models in comparison with experimental data outlines their relative merits: the coupled model provides the full solution for the solid surface cooling and for the droplet evaporation while the constant flux model predicts the transient surface temperature distribution reasonably well.

The multi-droplet model, which will be the subject of future studies, is based on the super-position of the transient surface thermal behavior due to a single evaporating droplet. Therefore, these two models provide the basis for its development.

Acknowledgements—This study was made possible by a grant of the Building and Fire Research Laboratory, National Institute of Standards and Technology. Partial funding of the computational expenditures was provided by the Computer Science Center of the University of Maryland at College Park.

REFERENCES

1. S. Toda, A study of mist cooling. First report: investigation of mist cooling, *Heat Transfer–Jap. Res.* 1(3), 39–50 (1972).
2. C. Bonacina, S. Del Giudice and G. Comini, Dropwise evaporation, *Trans. ASME, J. Heat Transfer* **101**, 441–446 (1979).
3. K. K. Tio and S. S. Sadhal, Thermal analysis of droplet spray evaporation from a heated solid surface, *Trans. ASME, J. Heat Transfer* **114**, 220–233 (1992).
4. S. Inada, Y. Mikasaka and K. Nishida, Transient heat transfer for a water drop impinging on a heated surface, *Bull. JSME* **28**(246), 2675–2681 (1985).
5. K. Makino and I. Michiyoshi, Effects of the initial size of water droplet on its evaporation on heated surfaces, *Int. J. Heat Mass Transfer* **22**, 979–981 (1979).
6. K. Makino and I. Michiyoshi, The behavior of a water droplet on heated surfaces, *Int. J. Heat Mass Transfer* **27**, 781–791 (1984).
7. T. Takano and K. Kobayashi, Vaporization behavior of a single droplet impinging on a heated surface with a flame-spayed ceramic coating, *Heat Transfer—Jap. Res.* **20**, 1–17 (1991).
8. S. Chandra and C. T. Avedisian, On the collision of a droplet with a solid surface, *Proc. R. Soc.* **432**, 13–41 (1991).
9. N. Zhang and W. J. Yang, Natural convection in evaporating minute drops, *Trans. ASME, J. Heat Transfer* **104**, 656–662 (1982).
10. T. Y. Xiong and M. C. Yuen, Evaporation of a liquid droplet on a hot plate, *Int. J. Heat Mass Transfer* **34**, 1881–1894 (1991).
11. M. Seki, H. Kawamura and K. Sanokawa, Transient temperature profile of a hot wall due to an impinging liquid droplet, *Trans. ASME, J. Heat Transfer* **100**, 167–169 (1978).
12. M. di Marzo and D. D. Evans, Evaporation of a water droplet deposited on a hot high thermal conductivity surface, *Trans. ASME, J. Heat Transfer* **111**, 210–213 (1989).
13. F. F. Simon and Y. Y. Hsu, Wetting dynamics of evaporating drops on various surfaces, *NASA TM X*-67913 (1971).
14. S. Ostrach and A. Pradhan, Surface-tension induced convection at reduced gravity, *AIAA J.* **16**(5), 419–424 (1978).
15. J. J. Rizza, A numerical solution to dropwise evaporation, *Trans. ASME, J. Heat Transfer* **103**, 501–507 (1981).
16. T. H. Chilton and A. P. Colburn, Mass transfer (absorption) coefficients prediction data on heat transfer fluid motion, *Ind. Engng Chem.* **26**, 1183–1187 (1934).
17. F. Kavoosi, M. di Marzo, H. R. Baum and D. D. Evans, An application of boundary element methods to a transient axisymmetric heat conduction problem, *ASME HTD* **110**, 79–85 (1989).
18. L. C. Wrobel and C. A. Brebbia, A formulation of the boundary element method for axisymmetric transient heat transfer conduction, *Int. J. Heat Mass Transfer* **24**, 843–850 (1981).
19. Y. Liao, Dropwise evaporative cooling of solid surfaces, Ph.D. Thesis, University of Maryland, College Park, Maryland (1992).
20. M. Klassen, M. di Marzo and J. Sirkis, Infrared thermography of dropwise evaporative cooling, *ASME HTD* **141**, 117–121 (1990).
21. M. Klassen and M. di Marzo, Transient cooling of a hot surface by droplets evaporation, *NIST-GCR* 90-575 (1990).
22. H. S. Carslaw and J. C. Jaeger, *Conduction of Heat in Solids*, pp. 214–217 and 264. Clarendon Press, Oxford (1959).